Science of the Total Environment 624 (2018) 638–647

Contents lists available at ScienceDirect

Science of the Total Environment

journal homepage: www.elsevier.com/locate/scitotenv

Turbidity composition and the relationship with microbial attachment and UV inactivation efficacy

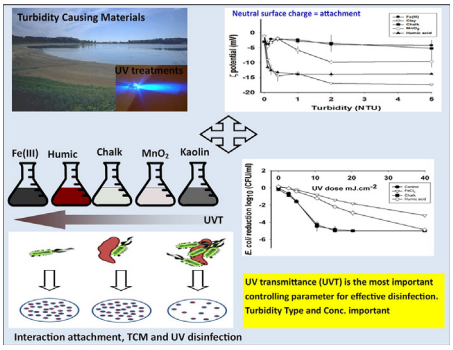
Charlotte Farrell [a,1], Francis Hassard [a,1], Bruce Jefferson [a], Tangui Leziart [a], Andreas Nocker [b], Peter Jarvis [a,*]

[a] Cranfield Water Science Institute, Cranfield University, Bedfordshire MK43 0AL, UK
[b] IWW Water Centre, Mülheim an der Ruhr, Germany

HIGHLIGHTS

- Impact of turbidity causing material (TCMs) on bacterial attachment and UV disinfection efficacy tested
- Neutral surface charge linked to attachment of bacteria to some TCMs
- *E. faecalis* more resistant than *E. coli* to UV disinfection
- UV transmittance most important for disinfection and TCMs have different transmittance
- The efficacy of uniform turbidity limits dependent on type and amount of turbidity

GRAPHICAL ABSTRACT



ARTICLE INFO

Article history:
Received 18 October 2017
Received in revised form 14 December 2017
Accepted 15 December 2017
Available online 27 December 2017

Keywords:
Water quality
UV disinfection
Inactivation
Faecal indicator organism
Turbidity
E. coli
E. faecalis

ABSTRACT

Turbidity in water can be caused by a range of different turbidity causing materials (TCM). Here the characteristics and attachment of bacteria to TCMs was assessed and the resultant impact on UV disinfection determined. TCMs represent potential vehicles for bacterial penetration of water treatment barriers, contamination of potable supplies and impact on subsequent human health. The TCMs under investigation were representative of those that may be present in surface and ground waters, both from the source and formed in the treatment process. The TCMs were chalk, Fe (III) hydroxide precipitate, kaolin clay, manganese dioxide and humic acids, at different turbidity levels representative of source waters (0, 0.1, 0.2, 0.4, 1, 2, and 5 NTU). *Escherichia coli* and *Enterococcus faecalis* attachment followed the order of Fe(III) > chalk, with little to no attachment seen for MnO_2, humic acids and clay. The attachment was postulated to be due to chalk and Fe(III) particles having a more neutral surface charge resulting in elevated aggregation with bacteria compared to other TCMs. The humic acids and Fe(III) were the TCMs which influenced inactivation of *E. coli* and *E. faecalis* due to decreasing UV transmittance (UVT) with increasing TCM concentration. The presence of the Fe(III) TCM at 0.2 NTU resulted in the poorest *E. coli* inactivation, with 2.5 $\log_{10}$ reduction at UV dose of 10 mJ cm^{-2} (k_d of -0.23 cm^2 mJ^{-1}) compared to a 3.9 $\log_{10}$ reduction in the absence of TCMs. *E. faecalis* had a greater resistance to UV irradiation than *E. coli* for all TCMs. Effective disinfection of drinking water is a priority for ensuring high public health standards. Uniform regulations for turbidity levels for waters pre-disinfection by UV light set by regulators may not always be appropriate and efficacy is dependent on the type, as well as the amount, of turbidity present in the water.

© 2018 The Authors. Published by Elsevier B.V. This is an open access article under the CC BY license (http://creativecommons.org/licenses/by/4.0/).

1. Introduction

Control of water quality presented prior to disinfection processes is of great importance to ensure that the water can be effectively treated

* Corresponding author.
E-mail address: p.jarvis@cranfield.ac.uk (P. Jarvis).
[1] These authors contributed equally to this work.

https://doi.org/10.1016/j.scitotenv.2017.12.173
0048-9697/© 2018 The Authors. Published by Elsevier B.V. This is an open access article under the CC BY license (http://creativecommons.org/licenses/by/4.0/).

and that water is safe at the point of use. The ability to kill or inactivate microorganisms largely depends on the water quality that is achieved at the end of the treatment process when disinfection is applied. Turbidity is one of the most widely used parameters for measuring water quality prior to disinfection. In Europe and the US, the regulatory requirement for water presented for disinfection and water post treatment is for a turbidity level of <1 NTU. The World Health Organisation (WHO) promotes an even lower turbidity threshold of below 0.2 NTU (WHO, 2011).

UV disinfection of drinking waters and wastewaters is expanding due to reduced formation of the currently regulated disinfection by products (DBP) and the high efficacy of UV irradiation against chlorine resistant pathogens such as *Cryptosporidium* and *Giardia* (Hijnen et al., 2006). The efficiency of UV disinfection is dependent on the turbidity of the water treated and the resultant transmittance of UV light through the water (Cantwell and Hofmann, 2011). There is therefore an important requirement to understand the impact of different turbidity causing materials (TCMs) on inactivation using UV irradiation.

TCMs can impact UV inactivation through various mechanisms, including scattering and absorption of incident UV light and through shielding of bacteria, protozoa and viruses, preventing sufficient UV dose for pathogen inactivation (Huber et al., 2011). TCMs can be comprised of many different types of material including natural organic matter (NOM), inorganic particles and biological particles (including bacteria and algae). Water treatment derived TCMs such as flocs formed from Al and Fe coagulants and naturally occurring TCMs, (such as NOM, clay and chalk) can both impact on water turbidity and be highly variable between source waters. Turbidity can arise during water treatment as dissolved substances may precipitate from the water phase. For example, coagulants are typically added resulting in the formation of precipitated flocs. Ineffective clarification processes may mean that metal hydroxide particulates are present in water which is presented for disinfection. Furthermore, as the pH of treated water may be raised through subsequent treatment processes, dissolved metals may again be encouraged to precipitate, thus increasing turbidity. In contrast, upland source waters often contain high concentrations of specific TCMs such as natural organic matter (NOM). Although NOM is predominantly dissolved, and not a true particle, its presence can still cause a turbidity signal and importantly have a UV absorbance or chlorine demand. Therefore, water with similar measured turbidity values can have different UV inactivation potential due to the type and concentration of TCMs (Passantino et al., 2004). Knowledge of TCM sub-components could question the validity of reported inactivation dose-response relationships of undesired microorganisms (Douterelo et al., 2016; Huber et al., 2011; Templeton et al., 2005) and challenge current guidelines on turbidity levels for treated waters or prior to UV disinfection.

Another important parameter influencing the inactivation of microorganisms is the potential for them to attach to the surface of particulate TCMs, or be bound together by large organic molecules, complexes of which can aggregate (Hess-Erga et al., 2008; Liu et al., 2013; Mamane, 2008; Wu et al., 2005). Attachment can add an additional layer of protection to microorganisms as a result of the proximity to the particulate matter, both by shading and, depending on the properties of the particulate, through absorbing incident UV light. Even greater protection can be provided through complete enclosure of microorganisms in the floc aggregates, which may be very resistant to UV penetration, principally due to their size. Microbial attachment to surfaces is driven by electrostatic interactions, van der Waals forces, hydrophobicity, surface tension and surface roughness (Hassard et al., 2016). The majority of bacteria and viruses are TCM-associated in soils and wastewater (Örmeci and Linden, 2002) however, the extent of TCM association in microbes within drinking systems is less clear (Liu et al., 2016). However, bacteria attached to particles have greater mobility in water than static biofilm bacteria and are potentially more resistant to inactivation than unattached planktonic bacteria (Liu et al., 2013, 2016). TCMs therefore, represent possible transmission vehicles for microbes through disinfection processes, which can lead to contamination of potable supplies by bacterial, protozoan or viral pathogens (Camper et al., 1986; Gall et al., 2015). Here model TCMs Fe(III), chalk, MnO_2, humic acids and clay were characterised and their impact on the aggregation behavior of bacteria was evaluated. Further, the impact of selected TCMs on the inactivation efficacy of different UV doses (0–39.9 mJ cm^{-2}) on key bacterial indicators (*E. coli* and *E. faecalis*) was then established.

2. Materials and methods

2.1. Bacterial growth and quantification

Experiments were performed with faecal indicator organisms, *E. coli* (ATCC 25922) and *E. faecalis* (ATCC 29212) as routinely measured compliance parameters for monitoring the microbial safety of drinking water. The gram-positive *E. faecalis* typically has greater resistance to stresses compared with the gram-negative *E. coli* (Anderson et al., 2005; Tree et al., 2003). Bacterial cultures were streaked from glycerol stocks on Trypticase Soy Agar (TSA) plates and grown at 37 °C for 24 h. Plates were then stored at 4 °C. A single colony was loop inoculated aseptically into 10 mL Tryptic Soy Broth (TSB, 10%) in a 50 mL centrifuge tube for *E. coli* and 10 mL TSB (35%) in an Erlenmeyer flask for *E. faecalis* followed by incubation at 30 °C on a rotary shaker (280 rpm). Different concentrations of TSB were used to ensure that the final optical density (OD_{600}) was equal to, or exceeded, a value of 1.0. The OD_{600} was determined using a spectrophotometer at 600 nm and adjusted to an OD_{600} of 1.0 using the same concentration of TSB as used for growth. The bacteria were harvested by centrifugation (5000*g*, 5 min) and resuspended in filtered (0.22 μm) mineral water (Evian, France). Washing was repeated twice prior to resuspension of bacteria in the original volume of mineral water. Samples were subsequently diluted to obtain working concentrations of 1×10^5 CFU/mL. Dilution factors were 10,000× for *E. coli* and 1200× for *E. faecalis*. Viable bacteria were quantified after UV treatment using a membrane filtration technique with averages calculated from appropriate serial dilutions (APHA-AWWA-WEF, 2012). All samples were serially diluted from 10^5 CFU/mL to 10^2 CFU/mL in microcentrifuge tubes (1.5 mL, Fisher Scientific, UK). The filter manifold (Combisart, Sartorius, UK) was heat-sterilised and prewashed with filtered mineral water (~5 mL). 1 mL of diluted sample was filtered onto sterile 0.22 μm cellulose filters (Fisher Scientific, UK) and filters were placed onto lactose glucuronide agar (MLGA; Oxoid, Fisher Scientific, UK) in the case of *E. coli* or MacConkey agar (Oxoid, Fisher Scientific, UK) in the case of *E. faecalis*. Plates were incubated at 37 °C for 24 h before enumeration.

2.2. Assimilable Organic Carbon (AOC) free glassware

AOC free glassware was prepared according to the method described in APHA-AWWA-WEF (2012). In brief, borosilicate glassware was machine-washed and rinsed three times with ultrapure (UP) water (Purelab Option – S7/15, 18.2MX cm and TOC <3 ppb). Glassware was incubated overnight in 0.2 M hydrochloric acid and rinsed with UP water. Glassware was air dried, covered with aluminum foil and incubated at 550 °C for 6 h in a muffle oven (Muffle Furnace 1400, PaveTesting Ltd., Hertfordshire, UK) and stored in a dry place away from sunlight until use. Teflon coated screw caps were washed with HCl as above and immersed into hot (60 °C) sodium persulphate solution (10%) for 1 h, rinsed 3 times with UP water and air dried. Glassware was stored in a dry place until use.

2.3. Preparation of TCM solutions

The TCMs selected represent a range of model suspended inorganic and organic materials found in drinking water sources and formed in the treatment process itself. Chalk (Fisher, CAT: C/1040/60), humic acids (Aldrich, CAT: H1675-2), manganese dioxide (Aldrich, CAT:

13242), kaolin clay (Aldrich, CAT: K7375) were obtained and used as supplied. Fe(III) hydroxide precipitate was produced by adding $FeCl_3$ (Aldrich, CAT: 15774-0) to UP water at a concentration of 25 mg/L at pH 4.5. The pH was subsequently adjusted to 7 using 0.1 M NaOH solution, the resulting Fe(III) hydroxide precipitate was washed three times in UP water, separated by centrifugation (1000 × *g*) and re-suspended in filtered mineral water. This Fe (III) hydroxide precipitate (henceforth Fe(III)) was subsequently used as the final TCM. Solutions of defined turbidities of these TCMs were prepared in 250 mL of filtered mineral water in AOC-free glass Erlenmeyer flasks. Stock solutions were made for each of the TCMs at a nephelometric turbidity level four-fold higher than the maximum working solution. Working TCM solutions were obtained by dilution of the concentrated stock solution. All solutions were made up to 100 mL using filtered mineral water, adjusted to pH 7 using HCl (0.1 M) or NaOH (0.1 M) to ensure that the osmotic balance of bacterial cultures was stable during the experiments. The water matrix pH was maintained at pH 7 to remain representative of typical final treated drinking waters and reduce experimental variables. The TCMs were prepared at turbidity values of 0, 0.1, 0.2, 0.4, 1, 2, and 5 NTU. Turbidity was measured using a Hach 2100 N turbidimeter. These turbidity ranges were chosen to cover the extremes of turbidity that may be experienced in source waters or prior to disinfection.

2.4. TCM characterisation

The particle size distribution was measured using a Malvern Mastersizer (Mastersizer 2000, Malvern Instruments Ltd., Malvern, UK) and particle count was assessed using a Spectrex analyser (PC-2200, Spectrex Corporation, USA). The UV light absorption of the sample was measured by spectrophotometry (Jenway 6715 UV, Dunmow, Essex, CM6 3LB) and the zeta potential (ζ) was measured using a zetasizer (Zetasizer Nano ZSP, Malvern Instruments Ltd., Malvern, UK). A field of 40 V was applied across an electrode spacing of 16 mm. Three repeat measurements on each sample were made to check the repeatability of the results obtained. The UV absorbance was measured by spectrophotometer at UV_{254} following standard method 5910 (APHA-AWWA-WEF, 2012).

2.5. Bacterial attachment to TCMs

Solutions of selected TCMs were prepared to 0.2 and 2 NTU in 99 mL of filtered mineral water at pH 7. The solution was stirred constantly using a magnetic stir bar and stirring plate at 250 rpm. The bacteria were diluted from a stock at 10^7 CFU/mL to the working concentration of 10^5 CFU/mL in both the control (0 NTU) and turbid solutions (0.2 and 2 NTU). All experiments were prepared in triplicate. 1 mL samples were taken directly after mixing bacterial cells with the TCM solution (time point zero, t = 0) and after 2 h (t = 2 h) of stirring to promote attachment. After 2 h, stirring was stopped to allow any particles, and particle-associated bacteria, to settle for 30 min prior to collection of another 1 mL sample (t = 2 h + set.). The bacteria were enumerated in the samples at t = 0, t = 2 and t = 2 h + set. by membrane filtration to assess the extent of *E. coli* and *E. faecalis* attachment and the settlement properties of the TCMs (Boulos et al., 1999). In these experiments, the pH was measured before and after the attachment assays, which in all cases confirmed that the pH did not change from pH 7. Therefore, attachment was predominantly linked to the different TCM properties and not water chemistry.

2.6. UV inactivation experiments

The UV inactivation experiments were carried out using a UVC-LED system consisting of a UVCLEAN lamp with multi-chip arrays of UV LEDs enclosed in a metal and glass housing from Sensor Electronic Technology (Columbia, South Carolina). UV light emitted by the LEDs was at a wavelength of 256 nm with a power output of 14 mW. A 25 mL Petri dish (50 mm × 12 mm) was used as the reactor and was placed under the lamps so that the system was completely illuminated. The reactor was continuously mixed with a magnetic stirrer. A 20 mL solution was placed in the Petri dish (comprising 19.8 mL TCM solution + 0.2 mL of bacterial suspension), which resulted in a UV path-length of 9.6 mm. Solutions of selected TCMs were prepared to 0.2 and 2 NTU in 19.8 mL of water at pH 7. In this set of experiments, the TCMs assessed for inactivation of *E. coli* and *E. faecalis* were Fe(III), chalk and humic acids. These were selected based on the results obtained from the TCM characterisation experiments. The solution was stirred continuously using a magnetic stirrer bar (mico, Fisher, UK) and stirring plate at 400 rpm. The bacteria were diluted from the initial stock suspension (10^7 CFU/mL) to the working concentration (10^5 CFU/mL) in both the control (0 NTU) and the turbid solutions (0.2 and 2 NTU). All experiments were undertaken in triplicate. Samples were exposed to 0, 2.8, 4.9, 10.5, 15.4 and 39.9 mJ cm^{-2} (0–48 minute incubation time). A radiometer (VLX-3W from Vilber Lourmat) was used to ensure the correct UV dose was applied to each sample.

2.7. UV inactivation kinetics of bacterial indicators

The efficacy of UV disinfection was described by inactivation kinetics. UV inactivation is defined as the reduction in the abundance of culturable bacteria (N), due to exposure to a UV dose and is commonly described by the first order disinfection model (Chick, 1908). The inactivation of bacterial indicators is described by the linear relationship between log inactivation and UV dose:

$$\log\left(\frac{N_t}{N}\right) = -k_d \times \text{UV dose} \quad (1)$$

where N_t is the bacterial concentration after contact time (t), UV dose (mJ cm^{-2}) is the product of the UV fluence rate (mW cm^{-2}) and the exposure (t) (Hijnen et al., 2006). The log N_t/N was assessed for the two-bacterial species at six UV doses for each TCM. k_d is the inactivation rate constant (cm^2 mJ^{-1}).

2.8. Statistical analysis

A two-way repeated measures ANOVA was used to determine the impact of TCM and UV dose on inactivation of *E. coli* and *E. faecalis*. The assumptions of ANOVA were met and the difference in the ANOVA was deemed significant at $p < 0.05$. Separate (for each species and TCM) hierarchical multiple linear regression analysis (MRA) was undertaken to understand the impact of each dependent variable (UV dose, UVT, ζ-potential, particle count, particle size, turbidity and attachment at t = 2 h + set) on the independent variables (UV inactivation of *E. coli* and *E. faecalis*). In all cases the assumptions of MRA were met and standardised regression coefficients (β coefficient) permitted comparison of the impact of dependent variables to each independent variable on the same scale (Germain et al., 2005). ANCOVA analysis was undertaken to differentiate between the effects of TCM type, attachment status (categorical predictor 0, 2 h, 2 h + set.) and TCM × attachment (interaction effect) on the bacterial concentration in the attachment microcosms.

3. Results and discussion

3.1. TCM characterisation

The particle size was similar across the turbidity ranges for most of the TCMs investigated. For MnO_2 and kaolin clay the median particle sizes were between 2 and 4.5 μm (Table 1). These results were consistent with the particle sizes measured previously for MnO_2 and kaolin particles (Luo, 2007; Murray, 2000). The Fe(III) particles increased in size from 3 to 6 μm as the turbidity increased between 0.1 and 5 NTU,

Table 1
ζ-Potential, particle size and particle counts and UV_{254} transmittance of TCMs at 2 NTU. (–) = data not applicable.

TCM	ζ-potential at pH 7 (mV)	Average particle size (μm)	Average particle counts/mL	UVT (%)
Chalk	−3.5 ± 2.8	2.8 ± 0.4	9138 ± 509	99.9
Fe(III)	−3.9 ± 0.1	4.2 ± 0.4	21,257 ± 3071	72.4
Humic acids	−13.9 ± 0.8	–	–	75.8
Clay	−17.2 ± 0.3	3.6 ± 1.1	29,458 ± 1411	99.9
MnO_2	−9.7 ± 0.6	2 ± 0.3	7199 ± 644	99.9

suggesting some aggregation was occurring at elevated Fe(III) particle concentration (Fig. 1A). The neutral surface charge of Fe(III) hydroxide particles (ζ-potential of 0 to ±5 mV) made these particles favourable for aggregation as a result of a low net energy barrier (Fig. 1B) (O'Brien and Hunter, 1981). At high turbidity, the high particle concentration increases the opportunity for particle-particle collisions in the Fe(III) system, increasing aggregation rates.

The same could have been expected for chalk which had a ζ-potential which was between 0 and 5 mV at pH 7, which is similar to previously reported values for chalk (Mahani et al., 2015). These particles carried minimal charge, suggesting that they may also aggregate under favourable mixing conditions, although this was not seen during the particle characterisation analysis here. The measured size range for chalk was 3–4 μm (Fig. 1A) which was consistent with that measured for calcite crystals (<5 μm) isolated from chalk soils (Kerry et al., 2009). The lack of aggregation suggests that other factors were controlling particle stability for chalk, such as a weak floc being formed that stabilised at a consistent particle size regardless of the particle concentration (Jarvis et al., 2005). Humic acids and clay on the other hand had more negative ζ-potential values (−10 mV) suggesting that these TCMs had a higher repulsive energy barrier and were unlikely to aggregate (Fig. 1B). The zeta potential profiles for all TCMs (from turbidity 0.1–5 NTU) showed increased negative charge with increasing turbidity. This may have been through accumulation of electrostatic surface charges due to greater particle surface area per volume (Quinlan and Tam, 2015) or possibly an artefact of measurement of zeta potential using laser Doppler electrophoresis (Kaszuba et al., 2010).

Consistent with the increase in turbidity, the particle counts increased with turbidity for all TCMs. Peng et al. (2009) demonstrated a strong positive relationship between light scattering (turbidity) and particle area and volume in environmental heterogenous populations of TCMs, which is consistent with the observations seen here. However, the particle concentrations were different between the TCMs for a given turbidity, in the order from greatest to least: clay > Fe(III) > MnO_2 = chalk (Fig. 1C). This illustrates that turbidity is dependent on multiple attributes of the particle population such as the physical and chemical composition, size distribution and particle shape. This means that particles of the same concentration may have very different values of turbidity. A material such as chalk which scatters light efficiently therefore requires fewer particles to scatter the same light as for a material such as iron hydroxide, which has poor scattering properties. As scattered light is directly proportional to the measured turbidity, the material properties will therefore influence the observed turbidity.

The increase in turbidity and particle concentration was not linear for all the TCMs, suggesting that the number of particles needed to increase the turbidity gets lower at higher turbidity levels for Fe(III) and clay (Fig. 1C). The relationship between concentration and turbidity

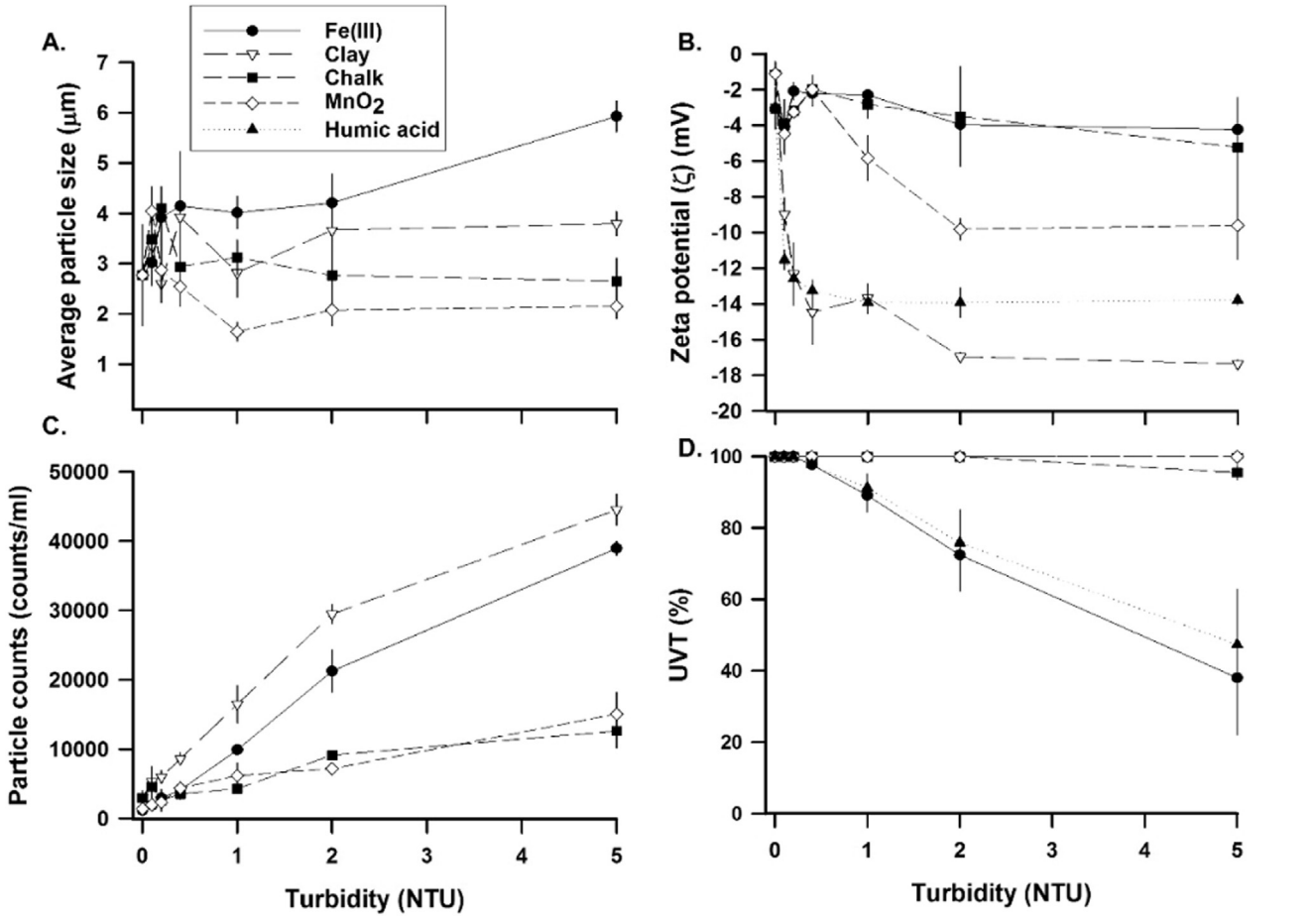


Fig. 1. A. TCM average particle sizes, B. Zeta (ζ)-potential of TCMs, C. Particle concentration of TCMs, D. UVT of TCMs at 254 nm. Data represent average ± 1 standard deviation. Particle size or particle counts were not measured in humic acids.

deviates from linearity for most TCMs above a turbidity value of >2 NTU. This was due to increased aggregation at higher turbidity (in the case of iron), omnidirectional re-radiation and increased likelihood of multiple scattering events at higher particle concentrations.

The TCMs exhibited differences in their absorbance of UV light at 254 nm. Fe(III) had a UVT of ~100% at 0.2 NTU which decreased to 38% UVT at 5 NTU (Fig. 1D). Humic acids also exhibited a high UV absorbance with UVT decreasing to 47% at 5 NTU. Clay, chalk and MnO_2 did not exhibit any significant UV_{254} absorbance across the studied turbidity range. Linear regression analysis revealed that at turbidity >0.4 NTU there was a ~12% decrease in UVT for every 1 NTU increase in turbidity for Fe(III) ($p < 0.001$) and humic acids ($p < 0.05$). Therefore, near complete obscuration (>99.9%) of incident UV_{254} was extrapolated to occur at 7.9 and 9.2 NTU for Fe(III) and humic acids respectively. In terms of UV obscuration, Fe(III) and humic acids therefore both represent significant risk factors in reducing critical UV doses required for bacterial inactivation. This suggests that different compositions of TCMs in water may have a greater impact on reducing UV disinfection efficacy through interaction with UV light or acting as pathogen carriers, despite identical turbidity.

3.2. Bacterial attachment to TCMs

3.2.1. Attachment

E. coli and *E. faecalis* attachment to different TCMs was measured at turbidity of 0.2 and 2 NTU. Recovered colony numbers after the addition of the TCM were compared with those of control samples without turbidity. Reduced colony numbers were taken to indicate bacteria-particle attachment, with >1 bacterium attaching to a particle or another bacterium on average. This enabled the calculation of TCM-bacteria concentration as a percentage of the control. The presence of the TCMs may have also inhibited the bacteria in other ways, although this was considered unlikely due to the inert nature of the TCM materials under test. There was no significant change in bacterial cell numbers between the control experiments, therefore relative change was examined between each TCM and attachment scenario. At $t = 0$ there was 102, 81 and 95% recovery of *E. coli* compared to the control for chalk, clay and humic acids at a turbidity of 0.2 NTU, suggesting little rapid attachment. If attachment was occurring, it was doing so based on a one-to-one ratio of particle and bacteria (Fig. 2A,B). There were similar concentrations of *E. coli* measured for MnO_2 compared to the control for both turbidity levels studied ($p < 0.05$), suggesting limited rapid attachment occurred for this TCM. *E. faecalis* had slightly lower concentration for chalk, clay and humic acid (~80% of those of the control without TCMs) at both 0.2 and 2 NTU at $t = 0$, whereas no initial change in bacterial numbers were seen for Fe(III) at both 0.2 and 2 NTU (Fig. 2B,D).

The presence of Fe(III) led to a reduction of colony counts for increasing exposure times to the TCMs particularly for *E. faecalis* (Fig. 2, $p = 0.015$ Table S1). For example, after 2 h of mixing, there was evidence of *E. coli* attachment to Fe(III), shown by reduced colony numbers of 69 and 86% at turbidity of 0.2 and 2 NTU respectively of those of the control without TCMs (Fig. 2C, E). The numbers of both *E. coli* and *E. faecalis* were very different for Fe(III) compared to other TCMs $p < 0.001$ in all cases (Table S1). However, the biggest difference in bacterial counts were seen for chalk at a turbidity of 2 NTU, where there were 50% of the *E. coli* colony numbers of those of the control without TCMs after 2 h, suggesting some attachment or inhibition had occurred. Only limited attachment (>90% numbers of those of the control without TCMs) was observed to have occurred at the lower turbidity of 0.2 NTU. Proposed attachment was typically greater at higher turbidity levels for most TCMs. For example, *E. faecalis* had 75% of the colony numbers of those of the control without TCMs at a chalk turbidity 0.2 NTU which further decreased to 50% colony numbers at 2 NTU. There was little or no attachment seen for MnO_2, humic acids or clay after 2 h of mixing (Fig. 2).

The Fe(III) TCM saw the most significant removal of bacteria from the water during the quiescent settlement phase, shown by the pairwise comparison between $t = 2 +$ set. and other attachment conditions (Table S1, $p < 0.001$). This was likely to be a result of enmeshment of bacteria as the precipitated iron hydroxides settled in the water, typical of a sweep flocculation mechanism. There were 51% of the colony numbers of *E. coli* compared to the control without TCMs from an experiment containing 0.2 NTU Fe(III) which decreased to 26% at 2 NTU, suggesting greater attachment during settlement as a result of the presence of more settling particles ($p = 0.028$). Similar observations were seen for the recovery of *E. faecalis* which reduced to 31 and 18% of those of a control without TCMs, after settlement for 0.2 and 2 NTU of Fe(III) respectively.

Across the study, the only significant attachment observed was for chalk and for Fe(III). For these particles, their neutral surface charge provides supporting evidence for the mechanism of attachment to the bacteria. For the other TCMs, with more negative surface charge, attachment was not likely to be favourable and if it was occurring then this was thought to be one-to-one attachment, due to the small changes in bacteria counts observed between the clay, MnO_2 and humic acids experiment and the controls which did not contain a TCM. Previous studies have estimated that up to 25–50 bacterial cells may attach to single particles, although this has been shown to vary between water and particle types (Liu et al., 2013). Bacterial attachment to surfaces is complex, particularly in the environment, where there are interactions between multiple bacteria, using signalling mechanisms such as quorum sensing (Emge et al., 2016). In addition, the background water matrix influences attachment mechanisms. However, here we have shown that a low magnitude of particle surface charge supports mechanisms for bacterial attachment. In addition, although shown to be limited here, particle association to TCMs introduces the potential for underestimation of bacterial abundance using widely used methods for enumeration, such as culturing on nutrient plates. In these methods bacterial colonies cannot be easily distinguished as having arisen from a single bacteria, aggregated bacteria or from bacteria attached to particles (Camper et al., 1986; Dietrich et al., 2007; Liu et al., 2016).

3.3. UV disinfection of E. coli and E. faecalis

3.3.1. Impact of TCMs

Fe(III), chalk and humic acids were selected for the disinfection tests as they represented materials which had high UV absorbance (humic acids and Fe(III)) and/or were shown to have the potential to attach with bacteria (Fe(III) and chalk). The *E. coli* log reduction at 0.2 NTU for Fe(III) increased from −0.4 to −4.3 as UV dose increased from 2.8 to 39.9 mJ cm^{-2} (Fig. 3A). The addition of Fe(III) significantly reduced the inactivation of *E. coli* with a k_d of −0.23 cm^2 mJ^{-1} for Fe(III) compared to a k_d of −0.31 cm^2 mJ^{-1} for the control at 0.2 NTU (Table 2; $p < 0.05$). At the higher turbidity of 2 NTU for Fe(III), the inactivation of *E. coli* (k_d) was 0.09 cm^2 mJ^{-1}, much lower than that seen at 0.2 NTU turbidity (k_d of −0.29 cm^2 mJ^{-1}, Table 2). Humic acids reduced the inactivation of *E. coli* compared to a control at turbidity of 2 NTU, as shown by a k_d value of −0.15 cm^2 mJ^{-1} ($p < 0.001$) compared to −0.29 cm^2 mJ^{-1} at 0.2 NTU. Chalk did not significantly impact the UV inactivation of either bacterial strain at the UV doses studied ($p > 0.05$). Overall, *E. faecalis* was more resistant to UV inactivation than *E. coli* in the presence of TCMs (Fig. 3), as only Fe(III) conferred protection at low turbidity with k_d of −0.03 cm^2 mJ^{-1} at 0.2 NTU (Table 2; $p = 0.001$), compared to other TCMs which had similar k_d values to the control (−0.31; $p > 0.05$). This could be due to structural proteins encoded by uvrA-like genes on plasmids, which enhance the resistance of some *E. faecalis* strains to the DNA damaging effects of UV light (Ozawa et al., 1997).

At the elevated turbidity, Fe(III) probably conferred greater protection from UV disinfection through the combined effects of having a low UVT (35% Fig. 1D) and offering some protection to bacteria through

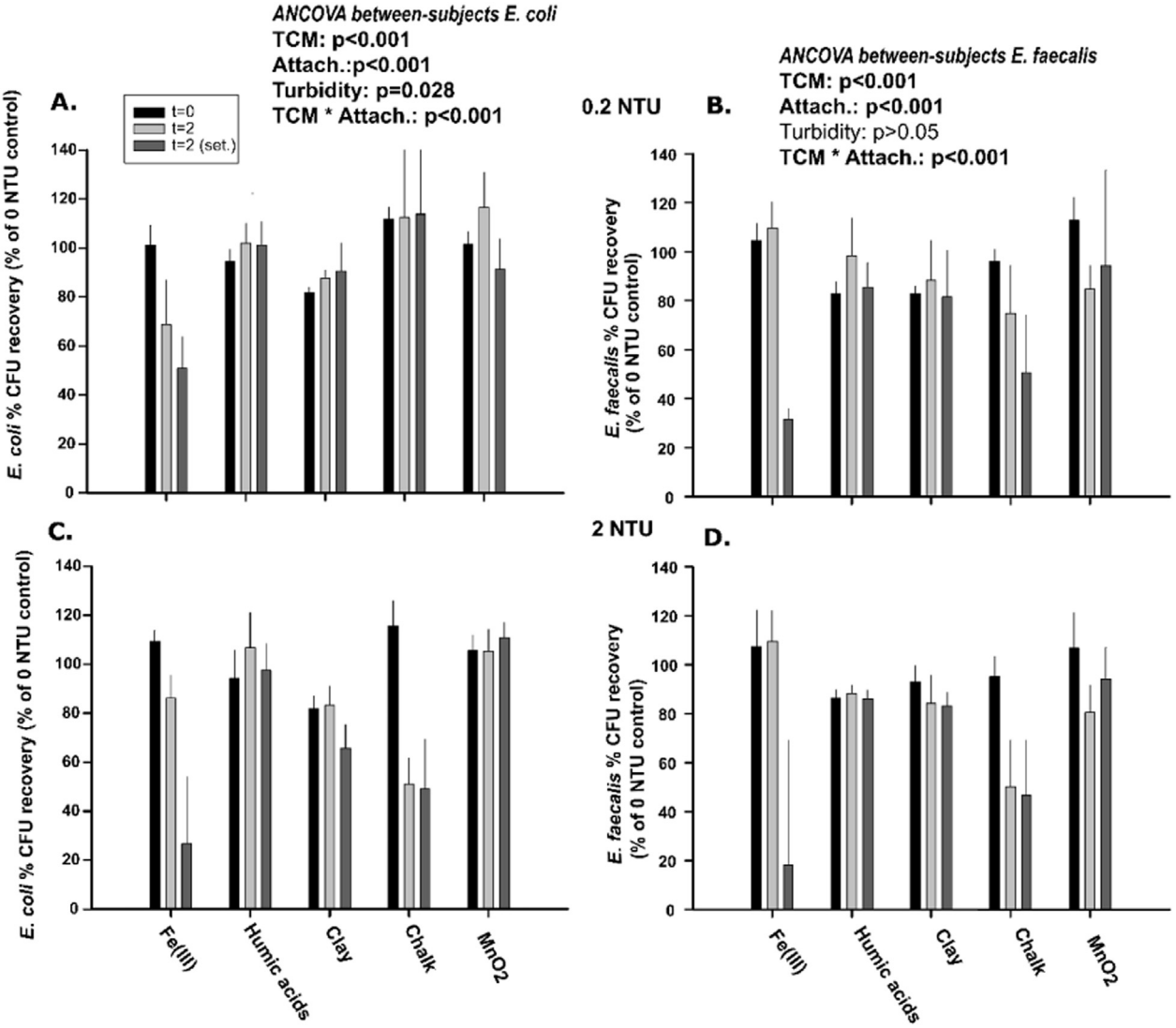


Fig. 2. Change of *E. coli* and *E. faecalis* concentration after period of mixing in microcosms containing different TCMs at 0.2 and 2 NTU compared to control experiments which did not contain TCMs A. *E. coli* at 0.2 NTU B. *E. faecalis* at 0.2 NTU C. *E. coli* at 2 NTU. D. *E. faecalis* at 2 NTU. t = time of mixing experiment (hours), t = 2 + set. represents the bacteria which could be recovered from the suspended phase after 2 h mixing and 30 min settlement. Bacteria were enumerated from the suspended phase therefore reduction of bacterial CFU from suspended phase suggests attachment. ANCOVA analysis of between subjects' effects is presented within graphs where bold text indicates significance at $p < 0.05$. Comprehensive ANCOVA report presented in Table S1.

attachment compared to other TCMs (Table 3, $\beta > 0.3$, $p < 0.05$). A similar trend was identified for humic acids, where only a small degree of attachment and settlement was seen (Table 3, $\beta = 0.26$, $p < 0.05$) but this material resulted in a low UVT (45%, Fig. 1D), which meant that the UV dose dominated impacted disinfection efficacy ($\beta = -0.88$, $p < 0.01$). Fe(III) coagulants are widely used in drinking water as the primary coagulants for particle removal. Ineffective clarification during water treatment or precipitation of naturally occurring soluble Fe in the source water could result in carryover of particulate Fe. However, iron coagulants have been widely implicated with poor UVT therefore reduced pathogen inactivation. These results confirm that the presence of iron particles, and also other strongly UB absorbing compounds such as humic acids, represent high risk factors relative to other types of turbidity in the success of UV disinfection (Kozak et al., 2010; Teunissen et al., 2008). In addition to providing photo-protective properties some, TCMs such as NOM, also increase regrowth potential in distribution systems as they represent direct substrates for bacterial growth. Other TCMs may also act as carriers of NOM through adsorption onto their surfaces leading to elevated biofilm growth rates and providing opportunities for bacterial re-growth following disinfection processes (Costerton et al., 1995; Douterelo et al., 2016). This further supports the minimisation of TCMs in drinking water.

3.3.2. Impact of UV dose

UV doses >15 mJ cm^{-2} were sufficient to achieve a 5 $\log_{10}$ *E. coli* inactivation at 0.2 NTU. Higher UV doses did not significantly improve inactivation of *E. coli* ($p > 0.05$) (Fig. 3A). In contrast, the maximum UV dose of 39.9 mJ cm^{-2} was required for complete *E. coli* inactivation in the presence of Fe(III) and humic acids ($p < 0.001$). The chalk TCM offered minimal UV protection as 5 $\log_{10}$ *E. coli* inactivation was observed at UV doses >10.5 mJ cm^{-2}. At turbidity of 0.2 NTU Fe(III), more than twice the UV dose was required for *E. faecalis* than *E. coli* to achieve a 3 $\log_{10}$ inactivation of bacteria. In the elevated turbidity experiments, the maximum inactivation was 2.4 and 3.5 $\log_{10}$ for *E. faecalis* at 39.9 mJ cm^{-2} for Fe(III) and humic acids respectively, which was ~1 $\log_{10}$ lower inactivation than at the lower turbidity of 0.2 NTU (Table 2). However, this was thought to be due to the inherent resistance of *E. faecalis* as opposed to attachment to Fe(III) particles as *E. faecalis* had 13% lower attachment than *E. coli* at this turbidity (Fig. 2). Other studies have demonstrated that the most UV resistant

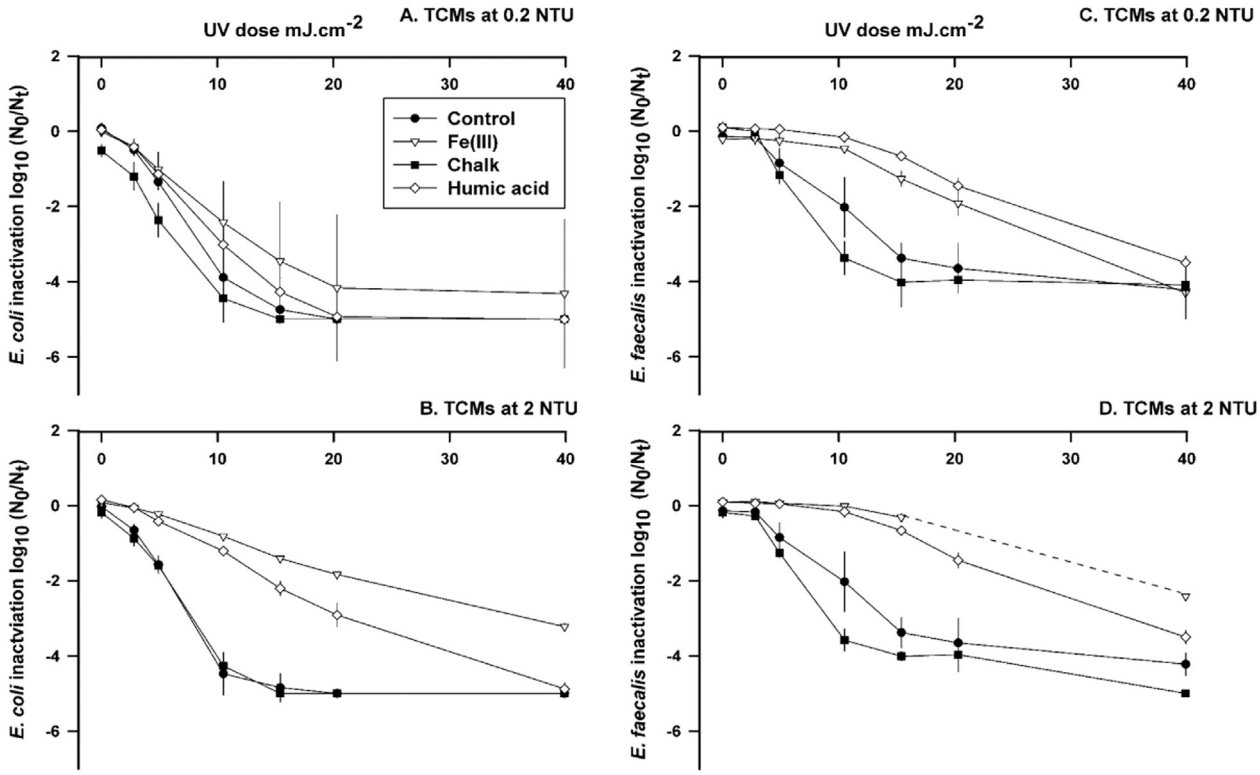


Fig. 3. UV dose on disinfection of bacterial indicators in the presence of TCMs at different turbidity A. *E. coli* 0.2 NTU, B. *E. coli* 2 NTU, C. *E. faecalis* 0.2 NTU and D. *E. faecalis* 2 NTU. Dashed line indicates missing data point.

organisms are viruses such as Adenoviruses with reported UV doses of up to 306 mJ cm^{-2} required to attain 6 log_{10} reductions (Hijnen et al., 2006). In this work 2.8-fold greater UV dose was required to attain a 4 log *E. coli* reduction at 2 NTU of Fe(III) compared to a control. Assuming a similar impact of turbidity on the log reductions for Adenovirus as *E. coli*, very high UV doses (>850 mJ cm^{-2}) may be required to attain 6 log reductions at 2 NTU of Fe(III) or humic acids. This is pertinent as water utilities are giving more attention to the effective treatment of viruses (Gall et al., 2015). Other studies have shown that *E. coli* has a ~5 log_{10} inactivation at UV doses of 9 mJ cm^{-2} using polychromatic UV sources (Oguma et al., 2002) and up to 15 mJ cm^{-2} using monochromatic UV sources (Hijnen et al., 2006). Therefore, even at the turbidity levels in water prior disinfection proposed by WHO (0.2 NTU), the UV dose required for equivalent 5 log_{10} inactivation was ~40 mJ cm^{-2} for Fe(III) and humic acid TCMs, while this was only 10.5 mJ cm^{-2} for chalk (Fig. 3). This highlights that UV disinfection efficacy is dependent on different bacteria, the concentration of particles, and the type of turbidity present.

The overall importance of UVT on disinfection was shown when considered independently of TCM. There was strong correlation between UVT and bacterial inactivation, independently of the TCM composition (Fig. 4). This was shown for both *E. coli* ($R^2 = -0.9$, $p = 0.01$) and *E. faecalis* ($R^2 = -0.83$, $p = 0.023$) based on averaged log inactivation. When considered by TCM type, the UV doses required for 3 log_{10} inactivation of *E. coli* were approximately double for Fe(III) and humic acids at 2 NTU (lower UVT) compared to 0.2 NTU (greater UVT) (Table 2). A UV dose of 14.7 mJ cm^{-2} for 0.2 NTU and 34.7 mJ cm^{-2} for 2 NTU was required for 3 log_{10} inactivation of *E. faecalis*. At the higher Fe(III) turbidity, 3 log_{10} inactivation of *E. faecalis* was not attained. Multiple regression analysis revealed that the UV dose governed most of the variability in *E. coli* ($\beta = -0.74$ $p < 0.001$) and *E. faecalis* ($\beta = -0.79$, $p < 0.001$) inactivation in the MLR model which contained all data based on the UVT of the TCMs. The importance of UV dose increased when considering Fe(III) ($\beta = -0.84$, $p < 0.001$) and humic acids ($\beta = -0.88$, $p < 0.001$) TCMs separately, highlighting the significant photoprotective properties of these TCMs.

Table 2
First order disinfection model for log_{10} inactivation of bacterial species at UV doses (0–39 mJ cm^{-2}) examined by linear regression analysis. Tailing of inactivation at higher UV doses were excluded from analysis.

Bacteria	TCMs	0.2 NTU			2 NTU		
		k_d cm^2 mJ^{-1} (R^2)	Max. inactivation (log_{10}) at 39.9 mJ cm^{-2}	UV dose for −3 log_{10} inactivation mJ cm^{-2}	k_d cm^2 mJ^{-1} (R^2)	Max. inactivation (log_{10}) at 39.9 mJ cm^{-2}	UV dose for −3 log_{10} inactivation mJ cm^{-2}
E. coli	Control (no TCM)	−0.31 (0.95)	−5	8.8	−0.44 (0.95)	−5	7.5
	Fe(III)	−0.23 (0.99)	−4.3	13.6	−0.09 (0.99)	−3.2	36.1
	Humic acid	−0.29 (0.99)	−5	10.6	−0.15 (0.99)	−4.8	21.2
	Chalk	−0.34 (0.99)	−5	7.1	−0.39 (0.98)	−5	8.1
E. faecalis	Control (no TCM)		−0.41 (0.97)	−4.2	−0.19 (0.94)	−4.2	3.04
	Fe(III)		−0.03 (0.86)	−4.3	−0.02 (0.88)	−2.4	(–)
	Humic acid		−0.41 (0.97)	−4.4	−0.05 (0.87)	−3.5	34.7
	Chalk		−0.59 (0.95)	−4	−0.34 (0.93)	−5	9.3

(–) indicates experimental conditions did not achieve 3 log_{10} inactivation.
UV dose for 3 log_{10} inactivation was calculated based on linear interpolation of plots of inactivation/UV dose.

Table 3
Multiple linear regression models to predict the role of TCM parameters and UV dose on disinfection of bacterial indicators *E. coli* and *E. faecalis*. A model containing all TCMs is presented. Each TCM was then modelled separately. Standardised β coefficients are reported with p value deemed significant at $p < 0.05$.

Model dependent variable→	Standardised β coefficient (p value)	
	E. coli inactivation	*E. faecalis* inactivation
Independent variables↓		
All TCMs included in model		
ζ-potential	0.22 (p = 0.93)	0.07 (p = 0.73)
Particle size	–	**0.30 (p = 0.01)**
Particle count	0.23 (p = 0.68)	−0.18 (p = 0.67)
UV dose	**−0.74 (p < 0.001)**	**−0.79 (p < 0.001)**
UVT	−0.05 (p = 0.98)	−0.32 (p = 0.27)
Turbidity	−0.04 (p = 0.79)	**0.31 (p = 0.03)**
Control model		
UV dose	**−0.77 (p = 0.03)**	**−0.79 (p = 0.01)**
Turbidity	0.02 (p = 0.94)	0.04 (p = 0.94)
Fe(III) model		
UV dose	**−0.84 (p < 0.001)**	**−0.82 (p < 0.001)**
Turbidity	0.39 (p = 0.07)	0.38 (p = 0.07)
Attachment t = 2 + set.	**0.39 (p < 0.01)**	**0.29 (p = 0.021)**
Chalk model		
UV dose	**−0.77 (p = 0.02)**	**−0.77 (p = 0.02)**
Turbidity	0.06 (p = 0.76)	0.06 (p = 0.76)
Attachment t = 2 + set. (settled)	0.06 (p = 0.75)	0.09 (p = 0.69)
Humic acids model		
UV dose	**−0.88 (p < 0.001)**	**−0.88 (p < 0.001)**
Turbidity	**0.26 (p = 0.04)**	–
Attachment t = 2 + set.[a]	**0.27 (p = 0.04)**	**0.26 (p = 0.04)**

Bold indicates variable that adds significant predictive value to the multiple linear regression model.
(–) indicates independent variable could not be included in the analysis. Variables excluded due to multi-collinearity are not presented.
[a] It was not possible to distinguish aggregation from attachment as humic acids result in aggregation and therefore turbidity and bacterial loss from suspension.

Attachment effects were small but important contributors influencing disinfection for some of the TCMs. Multiple regression analysis showed that bacterial attachment to Fe(III) was more important for preventing inactivation ($\beta = 0.39$, $p < 0.01$, Table 3) in *E. coli* compared to *E. faecalis* ($\beta = 0.29$, $p = 0.021$, Table 3) despite similar attachment rates (Fig. 2). This suggests the photo-protection afforded by TCMs could further increase the recalcitrance of more naturally resistant bacteria (demonstrated by lower β value for *E. faecalis* than *E. coli*) and interaction effect between TCM and attachment ($p < 0.001$). This could have important implications in water treatment particularly with respect to the significant role of settlement (Table S1, $p < 0.001$) when considering the emergence of pathogenic strains (Chiao et al., 2014).

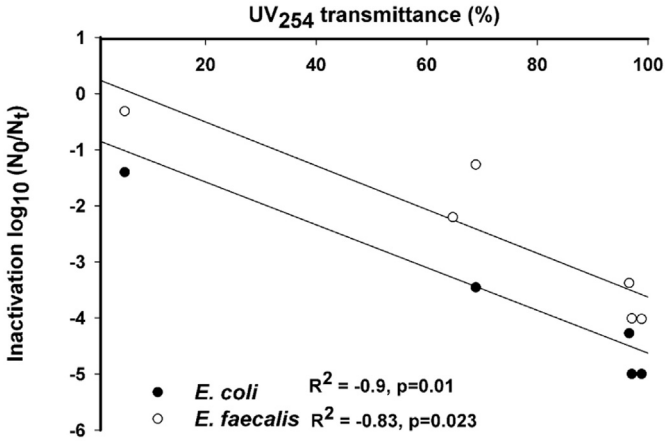


Fig. 4. Inactivation efficiency with UVT for *E. coli* and *E. faecalis*. Log_{10} reduction values were averaged across TCMs with similar % transmittance values.

Translation of these results to real water sources is complex due to the presence of multiple TCMs and background organic compounds, as well as opportunities for particle-surface conditioning by organic compounds such as proteins and humic/fulvic acids (Busscher et al., 1995; Gottenbos et al., 2001; van der Mei et al., 2008; Autin et al., 2013; Huber et al., 2011). However, these results show that knowledge of high risk TCMs in water prior to disinfection can enable public health engineers to adapt and modify treatment processes to the water quality. This research shows that mechanisms exist for bacteria to attach to some TCMs. This and, more importantly, the UV absorbing properties of the TCMs, results in significant impacts on UV disinfection efficacy. Particles such as Fe(III), that have a high UVT, and where there as evidence of attachment and aggregation with bacteria, are ideal transport vehicles to enable bacterial penetration through UV treatments. While both bacterial species displayed moderate attachment to chalk, particularly at high turbidity, the high UVT and poor photoprotective properties did not provide a protective benefit to bacteria from disinfection. The importance of UVT as the dominant control on disinfection efficacy was shown by humic acid, which didn't show significant attachment with bacteria, but had a big impact on overall disinfection efficacy.

The comparatively smaller impact of bacteria-particle association on disinfection may be explained by the relative sizes of bacteria to the sizes of the TCM particles of interest (Cantwell and Hofmann, 2011). This is important because it has been shown that some types of particle can protect much smaller microorganisms such as viruses from UV disinfection (Templeton et al., 2005). For example, association of bacteriophages MS2 and T4 to oxidized iron particles was shown to shield the viruses from UV light at a turbidity of 2.7 NTU. It has also been demonstrated that a shielding effect can occur when viruses were associated with humic acids and activated sludge flocs, whereas clay particles did not provide significant protection (Templeton et al., 2005). This is because clays and chalks typically scatter rather than absorb incident UV light, their impact on protecting microbes is much less (Bitton et al., 1972). This is in agreement with the results observed here where there was little to no impact of chalk on the disinfection of both *E. coli* and *E. faecalis*.

The relationship between turbidity and radiation dose has regularly been applied as a method to estimate dynamic decay rates in hydrodynamic models of faecal indicator bacteria (Kay et al., 2005; Whitehead et al., 2016). Data presented here suggests that turbidity significantly influences the survival of faecal bacteria exposed to incident UV light. Therefore, maximising UVT by minimising high risk TCMs is deemed critical for high UV inactivation efficacy and minimising public health risks. This basis of this research could be used to tailor the UV dose to the turbidity fingerprint of water prior to UV treatment as here it has been shown that the uniform turbidity recommendations for final treated waters set by some regulators may not be appropriate to promote sufficient disinfection for some types of turbidity.

4. Conclusions

Humic acids and Fe(III) most influenced disinfection of *E. coli* and *E. faecalis*. The reason was seen in the high UV_{254} of these two TCMs which increased with TCM concentration to 38% and 48% UVT at 5 NTU turbidity level. *E. coli* and *E. faecalis* attachment was only seen for chalk and Fe. The attachment was postulated to be as a result of these particles having a more neutral surface charge. The UV dose was the dominant mechanism governing >74% of the variability in *E. coli* and *E. faecalis* inactivation over a range of UV doses (0–39.9 mJ cm^{-2}, $p < 0.02$), irrespective of TCM. The presence of some TCMs substantially reduced the efficacy UV inactivation of *E. coli* for Fe(III) ($\beta = 0.39$) and humic acids ($\beta = 0.27$) with some of this attributed to attachment, but the majority due to reductions in UVT. Overall, *E. faecalis* was more resistant to UV inactivation in the presence of TCMs than *E. coli*

suggesting that the impact of TCMs could further increase the recalcitrance of more resistant strains reducing ability of UV to achieve statutory log reductions. Specific TCMs have significant photo-protective properties therefore they represent potential vehicles for bacterial penetration of water treatment barriers. Reducing carryover of Fe(III) and UV absorbing organic compounds to the disinfection stage is important as this TCM had both properties of light attenuation and flocculation. In conclusion, maximising UVT by minimising specific TCMs was critical for UV inactivation of bacterial indicators. Uniform regulatory turbidity levels for waters pre-disinfection set by regulators may not be appropriate depending on the TCM profile of the inlet water. To reduce the public health risk of particles and pathogens requires treatment which prioritises particle removal process upstream of effective disinfection of residual particles/pathogens.

Supplementary data to this article can be found online at https://doi.org/10.1016/j.scitotenv.2017.12.173.

Acknowledgements

This work was funded by the UK Water Industry Research Limited (UKWIR) under funding provision 16/DW/02/79. The authors were commissioned and funded by UKWIR to carry out this research, which was reported as a chapter presented within a technical report. The funding agency did not influence the content of this paper.

References

Anderson, K.L., Whitlock, J.E., Harwood, V.J., 2005. Persistence and differential survival of fecal indicator bacteria in subtropical waters and sediments. Appl. Environ. Microbiol. 71 (6):3041–3048. https://doi.org/10.1128/AEM.71.6.3041-3048.2005.

APHA-AWWA-WEF, 2012. Standard Methods for the Examination of Water and Wastewater. 22nd edition. (Washington).

Autin, O., Hart, J., Jarvis, P., Macadam, J., Parsons, S.A., Jefferson, B., 2013. The impact of background organic matter and alkalinity on the degradation of the pesticide metaldehyde by two advanced oxidation processes: UV/H_2O_2 and UV/TiO_2. Water Res. 47 (6):2041–2049. https://doi.org/10.1016/j.watres.2013.01.022.

Bitton, G., Henis, Y., Lahav, N., 1972. Effect of several clay minerals and humic acid on the survival of *Klebsiella aerogenes* exposed to ultraviolet irradiation. Appl. Microbiol. 23 (5), 870–874.

Boulos, L., Prevost, M., Barbeau, B., Coallier, J., Desjardins, R., 1999. LIVE/DEAD® Bac Light™: application of a new rapid staining method for direct enumeration of viable and total bacteria in drinking water. J. Microbiol. Methods 37, 77–86.

Busscher, H.J., Bos, R., van der Mei, H.C., 1995. Initial microbial adhesion is a determinant for the strength of biofilm adhesion. FEMS Microbiol. Lett. 128 (3), 229–234.

Camper, A.K., Lechevallier, M.W., Broadaway, S.C., Mcfeters, G.A., 1986. Bacteria associated with granular activated carbon particles in drinking water. Appl. Environ. Microbiol. 52 (3), 434–438.

Cantwell, R.E., Hofmann, R., 2011. Ultraviolet absorption properties of suspended particulate matter in untreated surface waters. Water Res. 45 (3):1322–1328. https://doi.org/10.1016/j.watres.2010.10.020.

Chiao, T.H., Clancy, T.M., Pinto, A., Xi, C., Raskin, L., 2014. Differential resistance of drinking water bacterial populations to monochloramine disinfection. Environ. Sci. Technol. 48 (7):4038–4047. https://doi.org/10.1021/es4055725.

Chick, H., 1908. An investigation of the laws of disinfection. J. Hyg. 8 (1):92–158. https://doi.org/10.1017/S0022172400006987.

Costerton, J.W., Lewandowski, Z., Caldwell, D.E., Korber, D.R., Lappin-Scott, H.M., 1995. Microbial biofilms. Annu. Rev. Microbiol. 49:711–745. https://doi.org/10.1146/annurev.mi.49.100195.003431.

Dietrich, J.P., Loge, F.J., Ginn, T.R., Başağaoğlu, H., 2007. Inactivation of particle-associated microorganisms in wastewater disinfection: modeling of ozone and chlorine reactive diffusive transport in polydispersed suspensions. Water Res. 41 (10):2189–2201. https://doi.org/10.1016/j.watres.2007.01.038.

Douterelo, I., Husband, S., Loza, V., Boxall, J., 2016. Dynamics of biofilm regrowth in drinking water distribution systems. Appl. Environ. Microbiol. 82:4155–4168. https://doi.org/10.1128/AEM.00109-16.

Emge, P., Moeller, J., Jang, H., Rusconi, R., Yawata, Y., Stocker, R., Vogel, V., 2016. Resilience of bacterial quorum sensing against fluid flow. Scientific Reports 6, 33115.

Gall, A.M., Mariñas, B.J., Lu, Y., Shisler, J.L., 2015. Waterborne viruses: a barrier to safe drinking water. PLoS Pathog. 11 (6), e1004867.

Germain, E., Stephenson, T., Pearce, P., 2005. Biomass characteristics and membrane aeration: toward a better understanding of membrane fouling in submerged membrane bioreactors (MBRs). Biotechnol. Bioeng. 90 (3):316–322. https://doi.org/10.1002/bit.20411.

Gottenbos, B., Grijpma, D.W., van der Mei, H.C., Feijen, J., Busscher, H.J., 2001. Antimicrobial effects of positively charged surfaces on adhering Gram-positive and Gram-negative bacteria. J. Antimicrob. Chemother. 48 (1):7–13 Retrieved from. http://www.ncbi.nlm.nih.gov/pubmed/11418507.

Hassard, F., Gwyther, C.L., Farkas, K., Andrews, A., Jones, V., Cox, B., Brett, H., Jones, D.L., McDonald, J.E., Malham, S.K., 2016. Abundance and distribution of enteric bacteria and viruses in coastal and estuarine sediments—a review. Front. Microbiol. https://doi.org/10.3389/fmicb.2016.01692.

Hess-Erga, O.K., Attramadal, K.J.K., Vadstein, O., 2008. Biotic and abiotic particles protect marine heterotrophic bacteria during UV and ozone disinfection. Aquat. Biol. 4 (2): 147–154. https://doi.org/10.3354/ab00105.

Hijnen, W.A.M., Beerendonk, E.F., Medema, G.J., 2006. Inactivation credit of UV radiation for viruses, bacteria and protozoan (oo)cysts in water: a review. Water Res. 40 (1): 3–22. https://doi.org/10.1016/j.watres.2005.10.030.

Huber, S.A., Balz, A., Abert, M., Pronk, W., 2011. Characterisation of aquatic humic and non-humic matter with size-exclusion chromatography - organic carbon detection - organic nitrogen detection (LC-OCD-OND). Water Res. 45 (2):879–885. https://doi.org/10.1016/j.watres.2010.09.023.

Jarvis, P., Jefferson, B., Gregory, J., Parsons, S.A., 2005. A review of floc strength and breakage. Water Res. 39:3121–3137. https://doi.org/10.1016/j.watres.2005.05.022.

Kaszuba, M., Corbett, J., Watson, F.M., Jones, A., 2010. High-concentration zeta potential measurements using light-scattering techniques. Philos. Transact. A Math. Phys. Eng. Sci. 368 (1927):4439–4451. https://doi.org/10.1098/rsta.2010.0175.

Kay, D., Stapleton, C.M., Wyer, M.D., McDonald, A.T., Crowther, J., Paul, N., Jones, K., Francis, C., Watkins, J., Wilkinson, J., Humphrey, N., Lin, B., Yang, L., Falconer, R.A., Gardner, S., 2005. Decay of intestinal enterococci concentrations in high-energy estuarine and coastal waters: towards real-time T90 values for modelling faecal indicators in recreational waters. Water Res. 39:655–667. https://doi.org/10.1016/j.watres.2004.11.014.

Kerry, R., Rawlins, B.G., Oliver, M.A., Lacinska, A.M., 2009. Problems with determining the particle size distribution of chalk soil and some of their implications. Geoderma 152 (3–4):324–337. https://doi.org/10.1016/j.geoderma.2009.06.018.

Kozak, J.A., Lordi, D.T., Abedin, Z., O'Connor, C., Granato, T., Kollias, L., 2010. The effect of ferric chloride addition for phosphorus removal on ultraviolet radiation disinfection of wastewater. Environ. Pract. 12 (4):275–284. https://doi.org/10.1017/S1466046610000487.

Liu, G., Ling, F.Q., Magic-Knezev, A., Liu, W.T., Verberk, J.Q.J.C., Van Dijk, J.C., 2013. Quantification and identification of particle-associated bacteria in unchlorinated drinking water from three treatment plants by cultivation-independent methods. Water Res. 47 (10):3523–3533. https://doi.org/10.1016/j.watres.2013.03.058.

Liu, G., Ling, F.Q., van der Mark, E.J., Zhang, X.D., Knezev, A., Verberk, J.Q.J.C., van der Meer, W.G.J., Medema, G.J., Liu, W.T., van Dijk, J.C., 2016. Comparison of particle-associated bacteria from a drinking water treatment plant and distribution reservoirs with different water sources. Sci. Rep. 6, 20367. https://doi.org/10.1038/srep20367.

Luo, Y., 2007. Preparation of MnO_2 nanoparticles by directly mixing potassium permanganate and polyelectrolyte aqueous solutions. Mater. Lett. 61 (8):1893–1895. https://doi.org/10.1016/j.matlet.2006.07.165.

Mahani, H., Keya, A.L., Berg, S., Nasralla, R., 2015. The effect of salinity, rock type and pH on the electrokinetics of carbonate-brine interface and surface complexation modeling. SPE Reservoir Characterisation and Simulation Conference and Exhibition. Society of Petroleum Engineers.

Mamane, H., 2008. Impact of particles on UV disinfection of water and wastewater effluents: a review. Rev. Chem. Eng. 24 (2–3):67. https://doi.org/10.1515/REVCE.2008.24.2-3.67.

van der Mei, H.C., Rustema-abbing, M., Langworthy, D.E., Collias, D.I., Mitchell, M.D., Bjorkquist, D.W., Busscher, H.J., 2008. Adhesion and viability of waterborne pathogens on p-DADMAC coatings. Biotechnol. Bioeng. 99 (1):165–169. https://doi.org/10.1002/bit.

Murray, H.H., 2000. Traditional and new applications for kaolin, smectite, and palygorskite: a general overview. Appl. Clay Sci. 17 (5–6):207–221. https://doi.org/10.1016/S0169-1317(00)00016-8.

O'Brien, R.W., Hunter, R.J., 1981. The electrophoretic mobility of large colloidal particles. Can. J. Chem. 59 (13):1878–1887. https://doi.org/10.1139/v81-280.

Oguma, K., Katayama, H., Ohgaki, S., 2002. Photoreactivation of *Escherichia coli* after low- or medium-pressure UV disinfection determined by an endonuclease sensitive site assay. Appl. Environ. Microbiol. 68 (12):6029–6035. https://doi.org/10.1128/AEM.68.12.6029-6035.2002.

Örmeci, B., Linden, K.G., 2002. Comparison of UV and chlorine inactivation of particle and non-particle associated coliform. Water Sci. Technol. Water Supply 2 (5–6):403–410. https://doi.org/10.2175/193864702785033923.

Ozawa, Y., Tanimoto, K., Fujimoto, S., Tomita, H., Ike, Y., 1997. Cloning and genetic analysis of the UV resistance determinant (uvr) encoded on the *Enterococcus faecalis* pheromone-responsive conjugative plasmid pAD1. J. Bacteriol. 179, 7468–7475.

Passantino, L., Malley, J., Knudson, M., Ward, R., Kim, J., 2004. Effect of low turbidity and algae on UV disinfection performance. J. Am. Water Works Assoc. 96 (6):128–137. https://doi.org/10.1108/17506200710779521.

Peng, F., Effler, S.W., Pierson, D.C., Smith, D.G., 2009. Light-scattering features of turbidity-causing particles in interconnected reservoir basins and a connecting stream. Water Res. 43 (8):2280–2292. https://doi.org/10.1016/j.watres.2009.02.018.

Quinlan, P.J., Tam, K.C., 2015. Water treatment technologies for the remediation of naphthenic acids in oil sands process-affected water. Chem. Eng. J. 279:696–714. https://doi.org/10.1016/j.cej.2015.05.062.

Templeton, M.R., Andrews, R.C., Hofmann, R., 2005. Inactivation of particle-associated viral surrogates by ultraviolet light. Water Res. 39 (15):3487–3500. https://doi.org/10.1016/j.watres.2005.06.010.

Teunissen, K., Abrahamse, A., Leijssen, H., Rietveld, L., van Dijk, H., 2008. Removal of both dissolved and particulate iron from groundwater. Drink. Water Eng. Sci. Discuss. 1 (1), 87–115.

Tree, J.A., Adams, M.R., Lees, D.N., 2003. Chlorination of indicator bacteria and viruses in primary sewage effluent. Appl. Environ. Microbiol. 69:2038–2043. https://doi.org/10.1128/AEM.69.4.2038.

Whitehead, P.G., Leckie, H., Rankinen, K., Butterfield, D., Futter, M.N., Bussi, G., 2016. An INCA model for pathogens in rivers and catchments: model structure, sensitivity analysis and application to the River Thames catchment, UK. Sci. Total Environ. 572:1601–1610. https://doi.org/10.1016/j.scitotenv.2016.01.128.

WHO, 2011. Guidelines for Drinking-water Quality. fourth edition. World Health Organization, Geneva (ISBN(9789241548151)).

Wu, Y., Clevenger, T., Deng, B., 2005. Impacts of goethite particles on UV disinfection of drinking water impacts of goethite particles on UV disinfection of drinking water. Appl. Environ. Microbiol. 71 (7):4140–4143. https://doi.org/10.1128/AEM.71.7.4140-4143.



https://dspace.org/

Turbidity composition and the relationship with microbial attachment and UV inactivation efficacy

Farrell, Charlotte; Hassard, Francis; Jefferson, Bruce; Léziart, Tangui; Nocker, Andreas ...

2017-12-27
Elsevier
https://doi.org/10.1016/j.scitotenv.2017.12.173
Farrell C, Hassard F, Jefferson B, (2018) Turbidity composition and the relationship with microbial attachment and UV inactivation efficacy. Science of the Total Environment, Volume 624, May 2018, pp. 638-647

Downloaded from a DSpace repository. https://dspace.org/